Available online at www.sciencedirect.com
ScienceDirect
Journal of Power Sources 172 (2007) 946–956
JOURNAL OF POWER SOURCES
www.elsevier.com/locate/jpowsour

ANN modeling of water consumption in the lead-acid batteries

Mohammad Ali Karimi [a,b,*], Hassan Karami [c], Maryam Mahdipour [a,d]

[a] Department of Chemistry, Payame-Noor University of Sirjan, Sirjan, Iran
[b] Department of Chemistry, Shahid Bahonar University of Kerman, Kerman, Iran
[c] Department of Chemistry, Payame-Noor University of Abhar, Abhar, Iran
[d] R&D Center, Sepahan Battery Industrial Complex, Oshtorjan Industrial Zone, Isfahan, Iran

Received 7 August 2006; received in revised form 31 May 2007; accepted 3 June 2007
Available online 21 June 2007

Abstract

Due to importance of the quantity of water loss in the life cycle of lead-acid batteries, water consumption tests were performed on 72 lead-acid batteries with low antimony grid alloy at different charge voltages and temperatures. Weight loss of batteries was measured during a period of 10 days. The behavior of batteries in different charge voltages and temperatures were modeled by artificial neural networks (ANNs) using MATLAB 7 media. Four temperatures were used in the training set, out of which three were used in prediction set and one in validation set. The network was trained by training and prediction data sets, and then was used for predicting water consumption in all three temperatures of prediction set. Finally, the network obtained was verified while being used in predicting water loss in defined temperatures of validation set. To achieve a better evaluation of the model ability, three models with different validation temperatures were used (model 1 = 50 °C, model 2 = 60 °C and model 3 = 70 °C). There was a good agreement between predicted and experimental results at prediction and validation sets for all the models.

Mean prediction errors in modeling charge voltage–temperature–time behavior in the water consumption quantity for models 1–3 were below 0.99%, 0.03%, and 0.76%, respectively. The model can be simply used by inexpert operators working in lead-acid battery industry.

Keywords: Water consumption; Artificial neural network; Model; Lead-acid batteries

1. Introduction

The two most common types of batteries widely used today are the sealed or maintenance-free lead–calcium battery and the low maintenance lead–antimony battery. The calcium or sealed battery uses less water and does not corrode nearly as much as the lead–antimony battery does. The lead–antimony battery (which mostly includes deep cycle batteries and batteries that have removable caps for adding water to battery cells) withstands continuous charge/discharge cycles and generally accepts charges more readily than a calcium battery. External corrosion problems associated with the sulfuric acid fumes being carried out of the battery by an extensive gas evolution due to electrolysis during charging [1].

To achieve long battery life, the lead–antimony battery requires frequent water additions to maintain proper electrolyte levels and the corrosion must be regularly removed from posts, cables, hold downs and battery trays.

Calcium is a mineral and antimony is a metal. The more antimony in the battery, the deeper discharge. However, the more antimony in a battery, the more gassing, corrosion and water consumption will be.

Some of the main reasons why batteries do not get full life cycles are corrosion, sulfation and water consumption [2–8]. The water level should never go beyond top border of plates and because of the presence of ingredients such as iron, chlorine etc. available in tap water always distilled water should be added and not tap water. If one battery is rated at a100 min reserve capacity and the plates in battery are 10 in. tall and water level gets 1 in. below the plate, this part of the plate will now dry out and becomes hard and at least 10% of batteries capacity just is lost while if water level gets 2 in. below the plate, at least 20% is lost. As a battery ages or gets older, it will lose some parts associated with charge acceptance and so it will use more water

* Corresponding author at: Department of Chemistry, Payame-Noor University of Sirjan, Sirjan, Iran. Tel.: +98 351 8252773; fax: +98 351 8253221.
E-mail addresses: m_karimi@pnu.ac.ir, ma_karimi43@yahoo.com (M.A. Karimi).

0378-7753/$ – see front matter © 2007 Elsevier B.V. All rights reserved.
doi:10.1016/j.jpowsour.2007.06.027

and thus it should be checked more frequently. Reduced charge acceptance is attributed to some different phenomena such as sulfation, passivation and other processes can also make some part of negative or positive paste inactive, so that at constant amount of charge coulombs, in old battery, more amount of electricity should be used for the electrolysis of water to realize the gas. But, at test time, there is not considerable change at amount of charge acceptance so; we do not attach a lot of importance to it in this model.

Because of the importance of water consumption especially in the antimony–lead-acid batteries and the necessity for its periodic determination and also long time spent on doing current available tests, we decided to use a model for calculating the amount of water loss in these batteries.

Being based on artificial neural network, this model can easily help the laboratory operator to control the water consumption at any time.

The basic units of neural networks, the artificial neurons, simulate the four basic functions of natural neurons. Various inputs to the network are represented by the mathematical symbol, $x(n)$. Each of these inputs is multiplied by a connection weight. These weights are represented by $w(n)$. In the simplest case, these products are simply summed, fed through a transfer function to generate a result, and then output. This process lends itself to physical implementation on a large scale and in a small package. This electronic implementation is still possible with other network structures which utilize different summing functions as well as different transfer functions. In currently available software packages these artificial neurons are called "processing elements" and have many more capabilities than the simple artificial neuron described above. Inputs enter into the processing element from the upper left. The first step is for each of these inputs to be multiplied by their respective weighting factor ($w(n)$). Then these modified inputs are fed into the summing function, which usually just sums these products. The output of the summing function is then sent into a transfer function. This function then turns this number into a real output via some algorithm. It is an algorithm that takes the input and turns it into a number like as 0, 1, −1 or some other. The transfer functions that are commonly supported are sigmoid, sine, hyperbolic tangent, etc. This transfer function can also scale the output or control its value via thresholds. The result of the transfer function is usually the direct output of the processing element. Finally, the processing element is ready to output the result of its transfer function. This output is then input into other processing elements, or to an outside connection, as dictated by the structure of the network.

Basically, all artificial neural networks have a similar structure or topology as shown in Fig. 1. In this structure, some of the neurons interface to the real world to receive its inputs. Other neurons provide the real world with the network's outputs. This output might be the particular character that the network thinks it has scanned or the particular image it thinks is being viewed. All the rest of the neurons are hidden from view [9].

There are many reports describing various attempts for utilizing various computational approaches to estimate the state of charge (SOC), cold cranking ability (CCA) and impedance modeling of intermediate size lead-acid batteries [10–19]. In

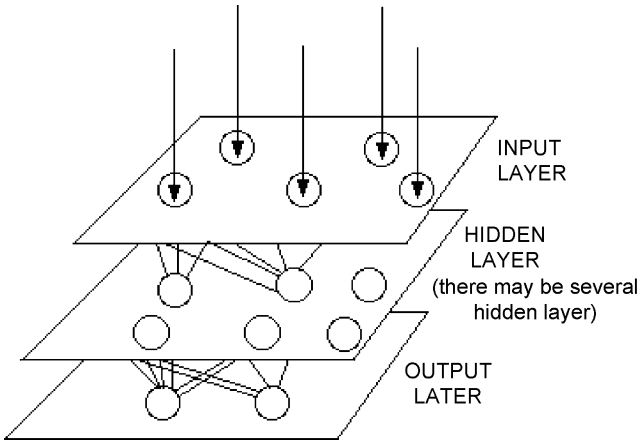

Fig. 1. A simple neural network diagram.

lead-acid batteries, water consumption is the most important process. Some processes including charge, overcharge and evaporation can reduce water content of the battery. It should be mentioned that water loss is one of the major processes which cause battery failure [4]. Therefore, simulation and modeling of water consumption in lead-acid batteries will be important and very interesting. However, to the best of our knowledge, no attempts has been made to model water consumption in lead-acid batteries.

In this paper, the water consumption computation model based on artificial neural network (ANN) for lead-acid batteries is introduced for the first time. The result of experiments proved further improvement of accuracy with the proposed model. Computation values are in good agreement with experimental data.

2. Experimental

2.1. Reagents and materials

All materials and reagents used in these experiments were industrial grade and all of them were obtained from Iranian companies. All lead-acid batteries 50 Ah used in the study were produced by Sepahan Battery Industrial Complex (Isfahan, Iran).

2.2. Instrumental

Provision of low temperature (0 °C) was carried out by industrial freezer (ARMDFB, Iran). Charging of batteries was performed by charge/discharge instrument (Moran, Italy). For determination of batteries weight, a balance with accuracy of 0.1 g was used (AND, Japan). A water bath (Pars Horm Co., Iran) was used for providing constant temperatures.

2.3. Methods

Six positive plates with the dimension of 107 mm × 143 mm (or total surface of 1836.12 cm^2 for two side surface of six positive plates) and five negative plates with the same dimension (or

Table 1
Water loss (g) experimental used data for modeling of water consumption in lead-acid batteries[a]

Temperature	Voltage								
	13	13.25	13.5	13.75	14	14.25	14. 5	14.75	15
0	16.8	17.8	20	23	26.7	30.4	32.5	35.6	37.8
30	35.3	40.6	48.9	55.2	59.2	61.6	69.3	75.4	89.5
40	66.6	71.8	77	85.2	90.3	95.3	100.2	105.7	111.4
50	82	92.2	103.6	109.5	113.7	118.3	123.4	128.8	134.3
60	102.1	111.6	122.4	129.6	135.2	140.1	146.3	151.9	155.7
70	129.1	135.3	145	152.1	158.3	165.6	170.8	176.1	182.1
80	147.6	152.5	160.2	169.2	176	183.4	189.9	197.2	206.4
90	169	179.8	190.5	198.2	206.6	211.5	218.4	226.6	234.6

[a] Final weights of batteries were measured after 140 h.

total surface of 1530.1 cm^2 for two side surface of five negative plates) were grouped to make a single block of 50 Ah and 12 V battery. The grids of all positive and negative plates were made from low antimony–lead alloy (1.7% Sb).

All low antimony–lead-acid batteries used in this study were the same in terms of open circuit voltage (OCV), weight, power and battery available capacity (BAC). Seventy-two batteries were introduced to eight different temperatures and nine different charge voltages were used for charging them. The lead-acid battery with nominal voltage of 12 V is used for exemplification, whose available capacity is 50 Ah at the 20 h discharge rate and temperature of 40 °C. For charging each battery one constant voltage was performed. Batteries were put in water baths with different temperatures. Hence at the end of the test program, all batteries has experienced nine different charge voltages and eight different temperatures. The experimental data has been shown in Table 1. It should be mentioned that only the final weights are shown in this table while the whole set of data is a collection of weights from every 5 h weight measurements of batteries. Based on the aforementioned conditions, the following test plans were performed during a period of 3 months and finally a complete set of data was collected. The procedure had the following steps:

1. Selection of 72 lead-acid batteries with the same open circuit voltage (OCV), weight, power and battery available capacity (BAC).
2. Charging the batteries using the same charge algorithm until they were fully charged.
3. Placing batteries in the freezer and different water baths to have constant different temperatures namely 0, 30, 40, 50, 60, 70, 80 and 90 °C (each battery was used only for one temperature).
4. At each temperature, charging the fully charged battery for 10 days at different constant voltages namely 13, 13.25, 13.5, 13.75, 14, 14.25, 14.5, 14.75 and 15 V (each battery was used only for one charge voltage).
5. The interval time for measuring the battery weight was 5 h and before each measurement, batteries were completely dried.
6. The obtained data during charge time were classified into three groups, and each group of data was separately modeled (Table 2).

Each network was established by four temperatures in training set and three temperatures in prediction set. The obtained models were used for prediction of the amount of water loss in prediction set and finally, they were validated by validation set. For increasing the accuracy and precision of the model, three networks were separately used for three selected dataset (Table 2). All steps of modeling were carried out in MATLAB 7 media.

It should be noted that in all linear and feed forward networks, log (weight) was used for modeling and this offered minimum error in the training and prediction dataset but a large error was obtained in the validation dataset. However, when the Elman (backward) network was tried with real target without any change, the amount of errors in all training, prediction and validation datasets were in the acceptable range.

To train the ANN model using the sigmoid transfer function, a learning process was carried out by adapting the connection weights in response to a number of training points of charge voltages and temperatures.

To optimize learning rate and momentum, the initial training of network was carried out by all data including training and prediction sets. Training of network was controlled by prediction error. After initial training, the model was trained without prediction set with the same learning rate and momentum for optimizing the weights and iterations. After this training, the obtained model was used for prediction of data in prediction set. This test is called internal validation. In the final step, the model was employed for prediction of data in validation set while this test is called as external validation.

The final model was used in MATLAB 7 media for making a file to be used by inexpert operators working in lead-acid battery industry.

Table 2
Selected temperatures (°C) for three networks as the three dataset[a]

Validation dataset	Prediction dataset	Training dataset	Parameter
50	0, 60, 80	30, 40, 70, 90	Network 1
60	40, 70, 90	0, 30, 50, 80	Network 2
70	30, 60, 80	0, 40, 50, 90	Network 3

[a] At each temperature, nine different voltages were used for charge (13, 13.25, 13.5, 13.75, 14, 14.25, 14.5, 14.75 and 15.0 V).

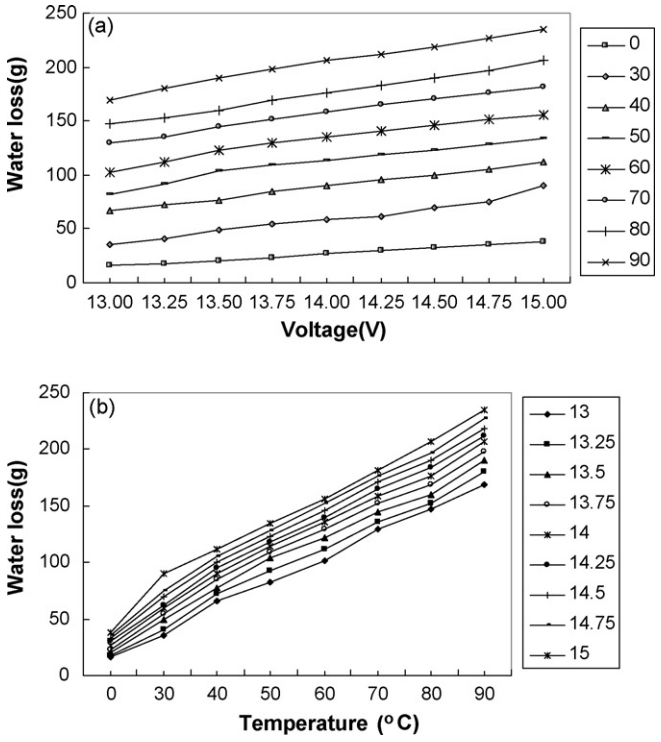

Fig. 2. Experimental data that monitors the relationship between temperature and voltage with quantity of water loss in the lead-acid batteries, (a) quantity of water loss in the constant voltages at the different temperatures (b) quantity of water loss in the constant temperatures at the different voltages.

3. Results and discussion

Water in a flooded lead-acid battery is lost as a result of evaporation and electrolysis into hydrogen and oxygen escaping into the atmosphere. One Faraday of overcharge will result in an electrolysis loss of about 18 g of water. Evaporation is a relatively small part of the loss except in very hot, dry climates. In a fully charged battery, electrolysis causes the water loss at a rate of 0.336 $cm^3\ Ah^{-1}$ overcharge. For example if a 500 Ah 12 V battery is overcharged about 10%, it can thus lose 16.8 cm^3 of its water during the test.

It is important that the electrolyte in a battery be maintained at proper level. The electrolyte not only serves as an ionic conductor, but also as a major factor in the transfer of heat from plates. If the electrolyte is below the plate level, then a part of the plate is not electrochemically efficient and this fact causes a concentration of heat in other parts of the battery. Periodic checking of water consumption can also serves as a rough check on charging efficiency and as a warning for the time when adjustment of the charger is required. Since replacing water can be seen as a major maintenance cost, water loss can be reduced by controlling the amount of overcharge and by using hydrogen and oxygen recombining devices in each cell where possible. Addition of water is best accomplished after recharge and before an equalization charge. Water is added at the end of the charge cycle to reach the high level line.

Realizing of gas during charge and overcharge will uniformly mix the water with the acid. In freezing weather, water should

Table 3
MSE status in the different training functions and in the different networks

Network type	Training function	Training parameters	MSE
Linear	LM	30 neurons and 30,000 epochs	1.0×10^{-3}
Feed forward	CGB	30 neurons and 1899 epochs	7.0×10^{-4}
	BFG	30 neurons and 3000 epochs	3.0×10^{-4}
	CGP	30 neurons and 758 epochs	1.0×10^{-3}
	CGF	30 neurons and 1360 epochs	9.0×10^{-4}
	GD	30 neurons and 3000 epochs	1.5×10^{-2}
	GDA	30 neurons and 3000 epochs	4.7×10^{-3}
	GDM	30 neurons and 3000 epochs	1.2×10^{-2}
	LM	3 neurons and 1451 epochs	1.5×10^{-3}
	LM	10 neurons and 2051 epochs	9.0×10^{-4}
	LM	30 neurons and 3000 epochs	2.6×10^{-4}
	LM	60 neurons and 3000 epochs	1.2×10^{-4}
	LM	60 neurons and 6000 epochs	1.0×10^{-4}
	OSS	30 neurons and 3000 epochs	9.9×10^{-4}
	SCG	30 neurons and 3000 epochs	7.0×10^{-4}
Backward (Elman)	GDM	10 neurons and 30,000 epochs	7.0×10^{-4}
	LM	10 neurons and 10,000 epochs	1.0×10^{-4}
	GDX	30 neurons and 10,000 epochs	9.0×10^{-4}
	GDX	10 neurons and 10,000 epochs	4.0×10^{-4}

Table 4
Descriptions of the training functions

Training functions	
trainb	Batch training with weight and bias learning rules
trainbfg	BFGS quasi-Newton back propagation
trainbr	Bayesian regularization
trainc	Cyclical order incremental update
traincgb	Powell–Beale conjugate gradient backpropagation
traincgf	Fletcher–Powell conjugate gradient, backpropagation
traincgp	Polak–Ribiere conjugate gradient backpropagation
traingd	Gradient descent backpropagation
traingda	Gradient descent with adaptive lr backpropagation
traingdm	Gradient descent with momentum backpropagation
traingdx	Gradient descent with momentum & adaptive lr backprop
trainlin	Levenberg–Marquardt backpropagation
trainoss	One step secant backpropagation
trainr	Random order incremental update
trainrp	Resilient backpropagation (Rprop)
trains	Sequential order incremental update
trainscg	Scaled conjugate gradient backpropagation

Table 5
Architecture and specification of the generated ANNs

Network	1,2,3
No. of input layers	3
No. of hidden layers	2
No. of neurons in the hidden layers	10
No. of output layers	1
Learning rate	0.1
Momentum	0.1
Number of epochs	10,000
Transfer function	Tangent sigmoid

Networks 1, 2 and 3 were used for water consumption behavior at different constant charge voltages and temperatures.

not be added without mixing as it may freeze before gassing process occurs. Therefore, the added water should be mechanically mixed with residual electrolyte in the battery, e.g. by shaking of the battery. Although demineralized water may be acceptable for some batteries, the low cost of distilled water makes it the best choice.

Overfilling must be avoided as the resultant overflow of acid electrolyte will cause tray corrosion, ground paths, and loss of cell capacity. Although distilled water is no longer specified by most battery manufacturers; good quality water, low in minerals and heavy metal ions such as iron, will help prolong battery life.

Water loss is one of the major causes of battery failure [4]. When water in battery acid evaporates, lead plates are exposed to air and can corrode because the irreversible lead oxide on the negative plates is produced when exposed to air. Also the positive plates are sulfated with residual sulfuric acid which is remained on the surface of them. This process is often reversible unless deep sulfation is produced.

For the first time, we represent the modeling of water consumption in the lead-acid batteries to achieve the best and fast way of water loss determination in the manufacturing companies (the standard test of water loss takes a long time depending on the standard type (21–62 days)). For example, in Iranian

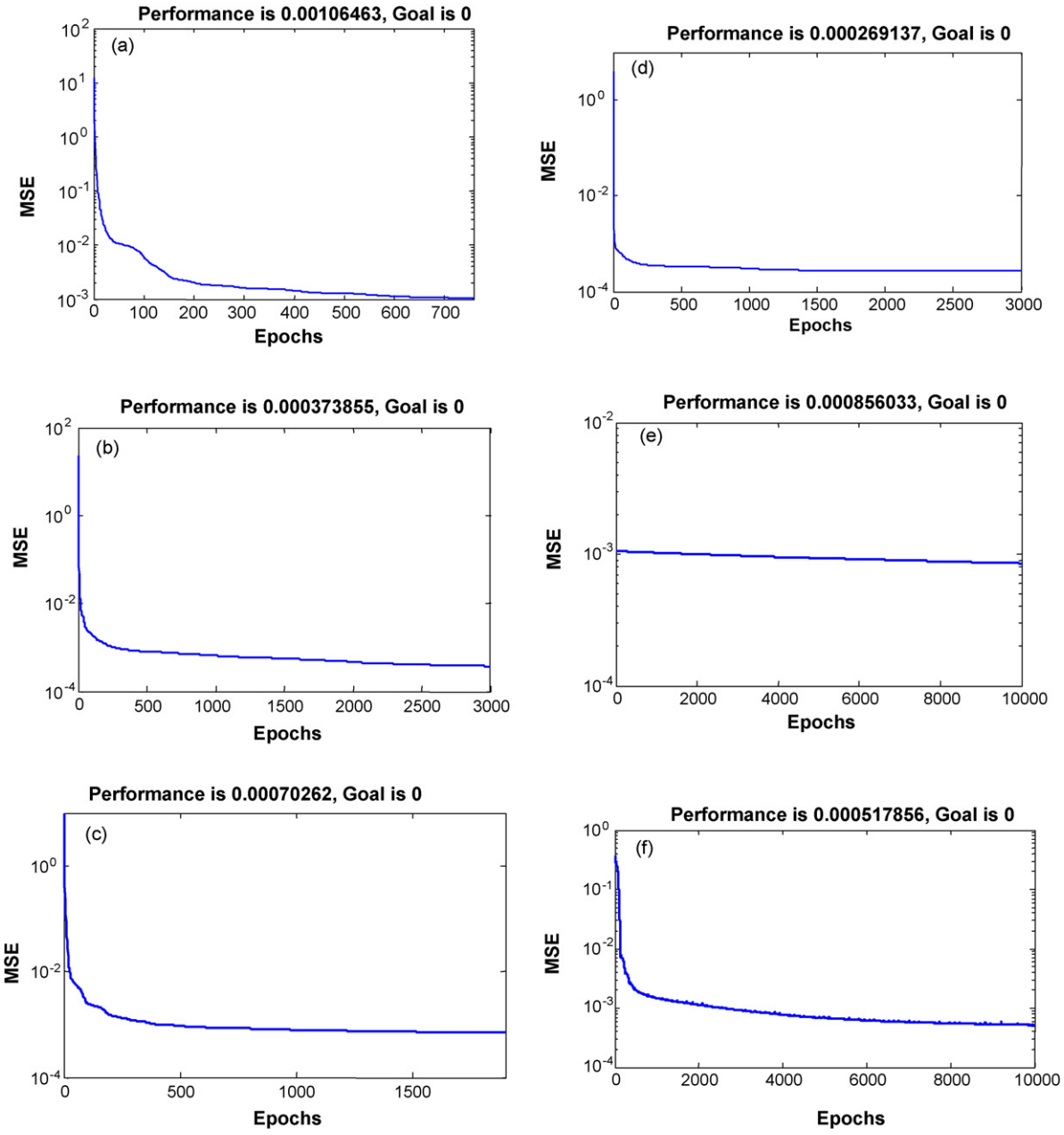

Fig. 3. The relationship between MSE and number of epochs in the different training functions, (a) train-cgp with 30 neurons and feed forward net, (b) train-bfg with 30 neurons and feed forward net, (c) train-cgb with 30 neurons and feed forward net, (d) train-lm with 30 neurons and feed forward net, (e) train-gdm with 10 neurons and Elman net, (f) train-gdx with 10 neurons and Elman net.

national standard [20] and IEC [21] the following test procedure and critical conditions are used for water consumption test, respectively:

1. Charging batteries for 21 days with a constant voltage of 14.4 V at 40 °C, and determination of weight difference. In this procedure the ratio of the amount of water loss to the capacity of batteries should be less than 6 g Ah^{-1} for antimony batteries.
2. Charging batteries for 500 h with a constant voltage of 14.4 V at 40 °C, and measuring the weight (W_1) and continuing the charge condition for another 1000 h and getting the W_2. In this procedure the amount of water loss $[(W_2 - W_1)/2]$ divided by capacity of batteries should be less than 1 g Ah^{-1} for antimony batteries.

Because of the fact that in majority of international quality control standards and quality control centers for lead-acid industries, all water consumption tests for vehicle batteries are carried out at a constant charge voltage and temperature, in this work, water consumption is discussed in different constant charge voltages and temperatures.

The water consumption quantity is attributed to grid design (available surface area), grid alloy, electrolyte level (upper than plates or lower than them), paste composition, ambient temperature and charge voltage. For this reason we limited our variables and used the same batteries in the case of grid design, grid alloy, level of electrolyte and all of the related parameters and only the temperature and voltage of charge were changed.

During the test, the major part of charge is consumed only in electrolysis, and other processes including corrosion, capacity recharge due to self-discharge, and on the other side reactions during test time are trivial. For example, batteries used in the test have less than 1% self-discharge per day and therefore, 0.5 Ah can be reduced from total capacity of a 50 Ah–12 V battery. A few minutes of charging can compensate for this amount of self-discharge.

To collect the data, all batteries were charged at different constant voltages (V) and temperatures for 10 days. Because of this fact that in cold temperatures, water loss occurs only from electrolysis, 0 °C was selected to study the behavior of batteries in these climates. Because of time-consuming behavior of experiments, we used only eight temperatures for experiences and thus, we could use only one temperature in validation set. Therefore, for validation of the model, three networks with different groups of dataset were trained. This classification is shown in the Table 2. The results showed that in all networks, the model has the same behavior and this could verify the strength of this model. It should be mentioned that the model was trained by using log (w) in the Feed forward network and real (w) was used in the Elman network.

We posited that while increasing the temperature and charge voltages, the quantity of water loss increases and as it is seen

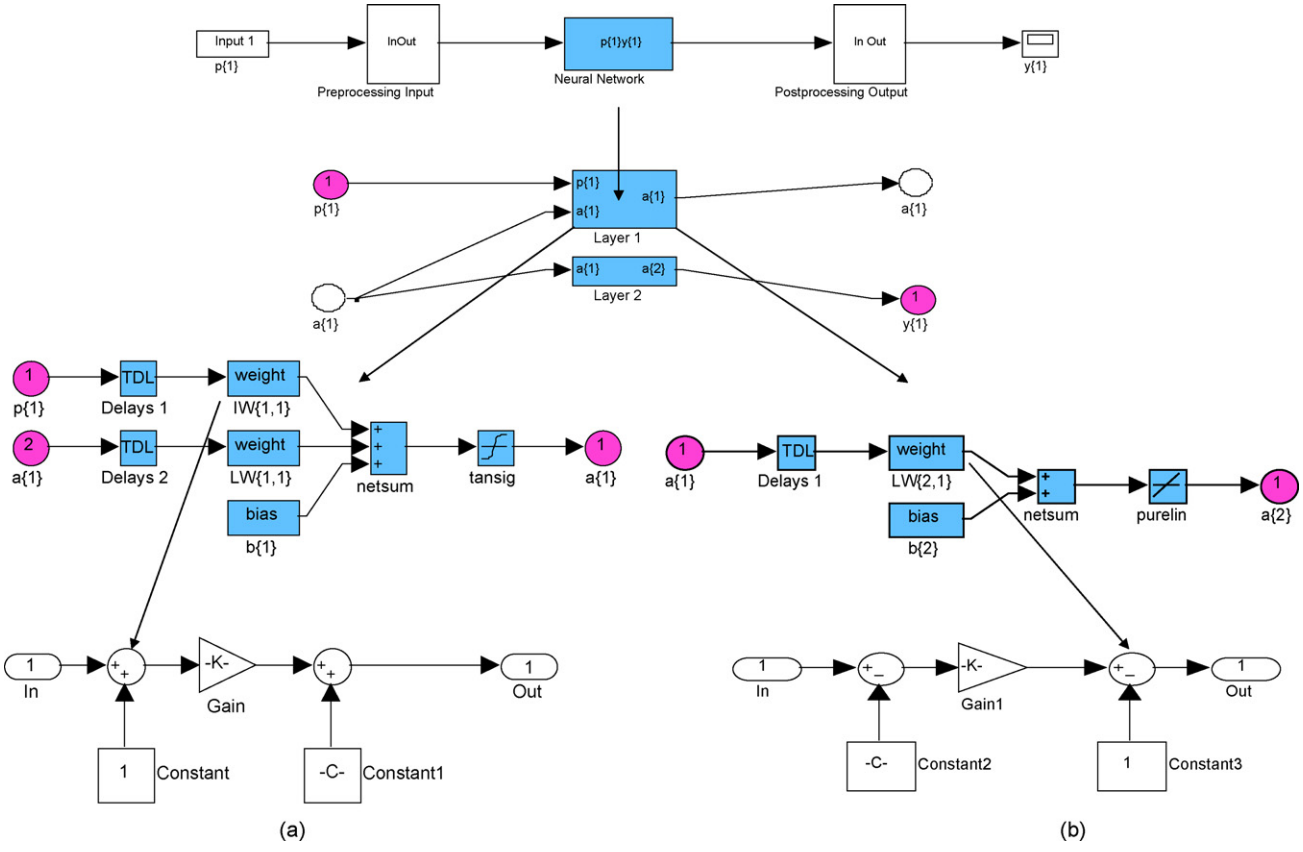

Fig. 4. The schematic of final model (a) preprocessing input (b) postprocessing output (c) weights.

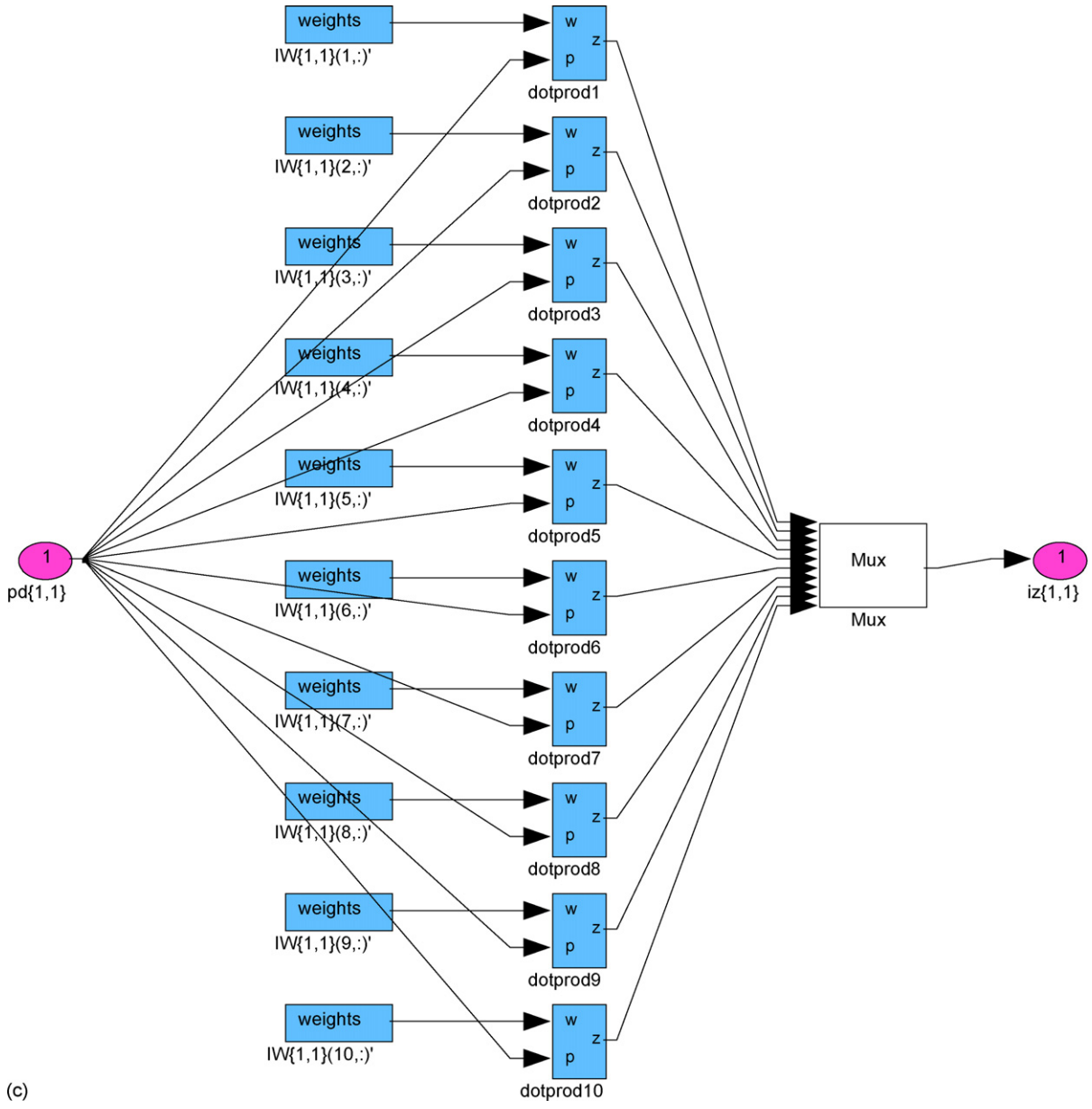

Fig. 4. (*Continued*).

from Fig. 2, the experimental data shows this proportional relationship and supports the idea.

Table 3 shows the comparison between different training functions and as it is shown the "train-lm" function had the best performance and as a result with less MSE (Mean Square Error) in both Feed forward and Elman networks but the prediction error in the Elman network was more while using this function and due to this reason we used the "train-gdx" function for Elman network. Table 4 shows a brief description of training functions listed in Table 3. Fig. 3 shows the relationship between MSE and number of epochs in different training functions in network 1. As it is seen from this figure, the performance of train-lm function in the feed forward network (Fig. 3d) is lower than other functions which mean that it has a lower mean square error. However, as it was mentioned before, we had a high prediction error with this network and because of this, the Elman network was used with train-gdx function in the training process. As it is seen from Fig. 3f, it has a low MSE. The prediction error was used as a tool for controlling the training process. The model with the lowest prediction error was used as final and optimum model. Table 5 shows the architectures and specifications of the optimized ANN (for three networks). The schematic of network is shown in Fig. 4. After training process, it was used for prediction of water consumption quantity in the batteries at three different temperatures in the prediction set as an internal validation. Fig. 5 shows variation of the predicted data versus experimental data in prediction set of network 1 at 0–140 h for different constant temperatures and voltages.

Variations of predicted data versus experimental data for networks 2 and 3 in prediction set at 0–140 h for different constant temperatures and voltages are shown in Figs. 6 and 7. As it is seen from these figures, the prediction data has a good compat-

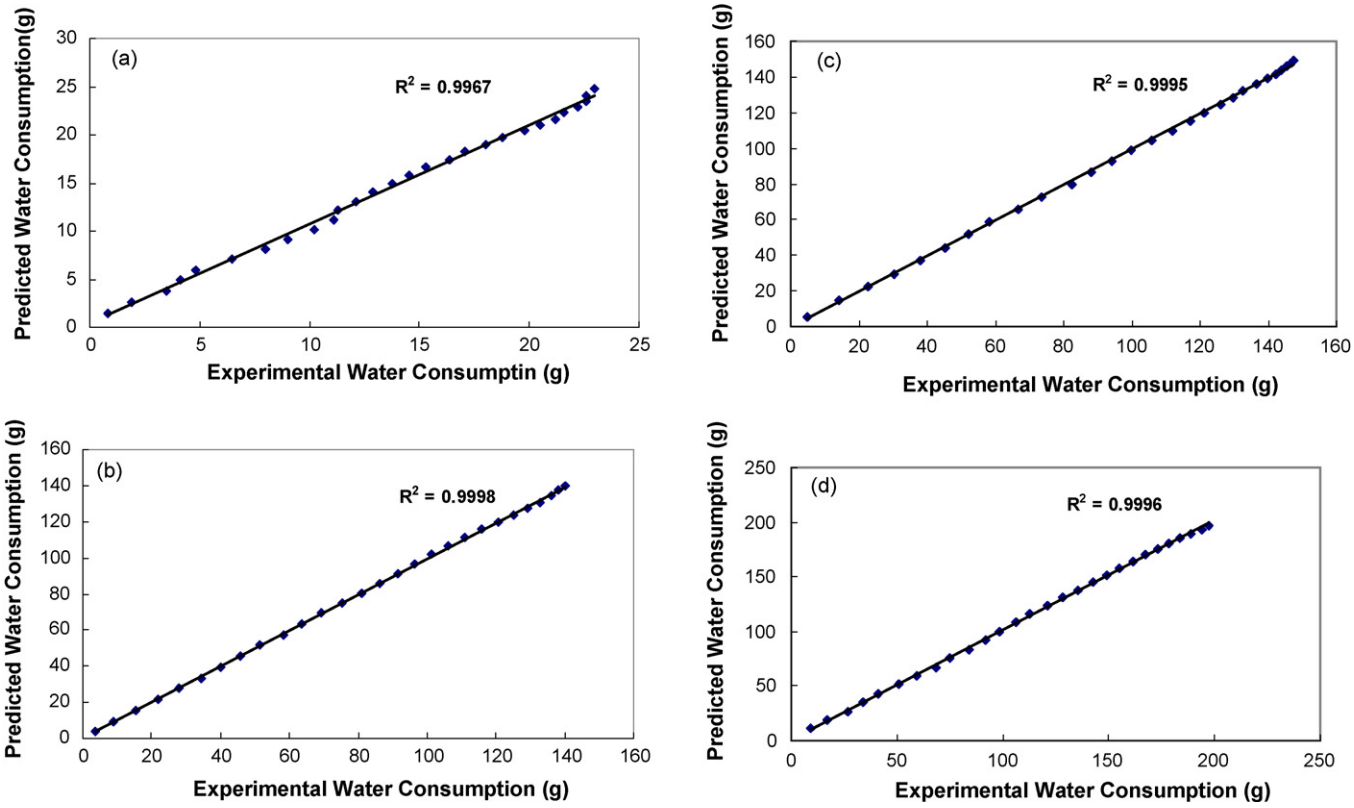

Fig. 5. Variation of predicted weights (water consumption quantity) vs. experimental weights (water consumption quantity) at 0–140 h for constant temperatures and voltages of (a) 0 °C and 13.75 V, (b) 60 °C and 14.25 V, (c) 80 °C and 13 V, (d) 80 °C and 14.75 V for network 1 in prediction set.

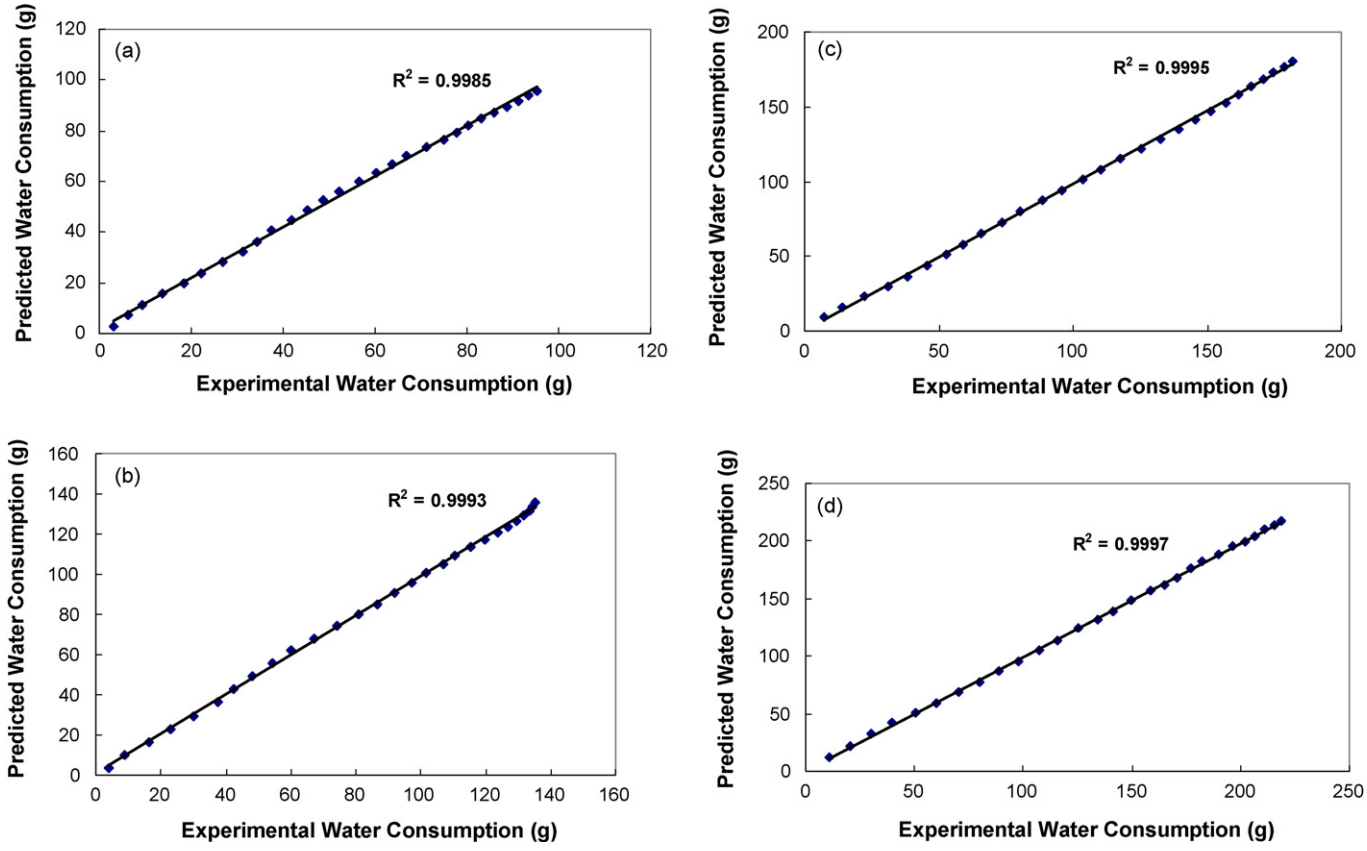

Fig. 6. Variations of predicted weights (water consumption quantity) vs. experimental weights (water consumption quantity) for network 2 in prediction set at 0–140 h for constant temperatures and voltages of (a) 40 °C and 14.25 V, (b) 70 °C and 13.25 V, (c) 70 °C and 15 V, (d) 90 °C and 14.5 V.

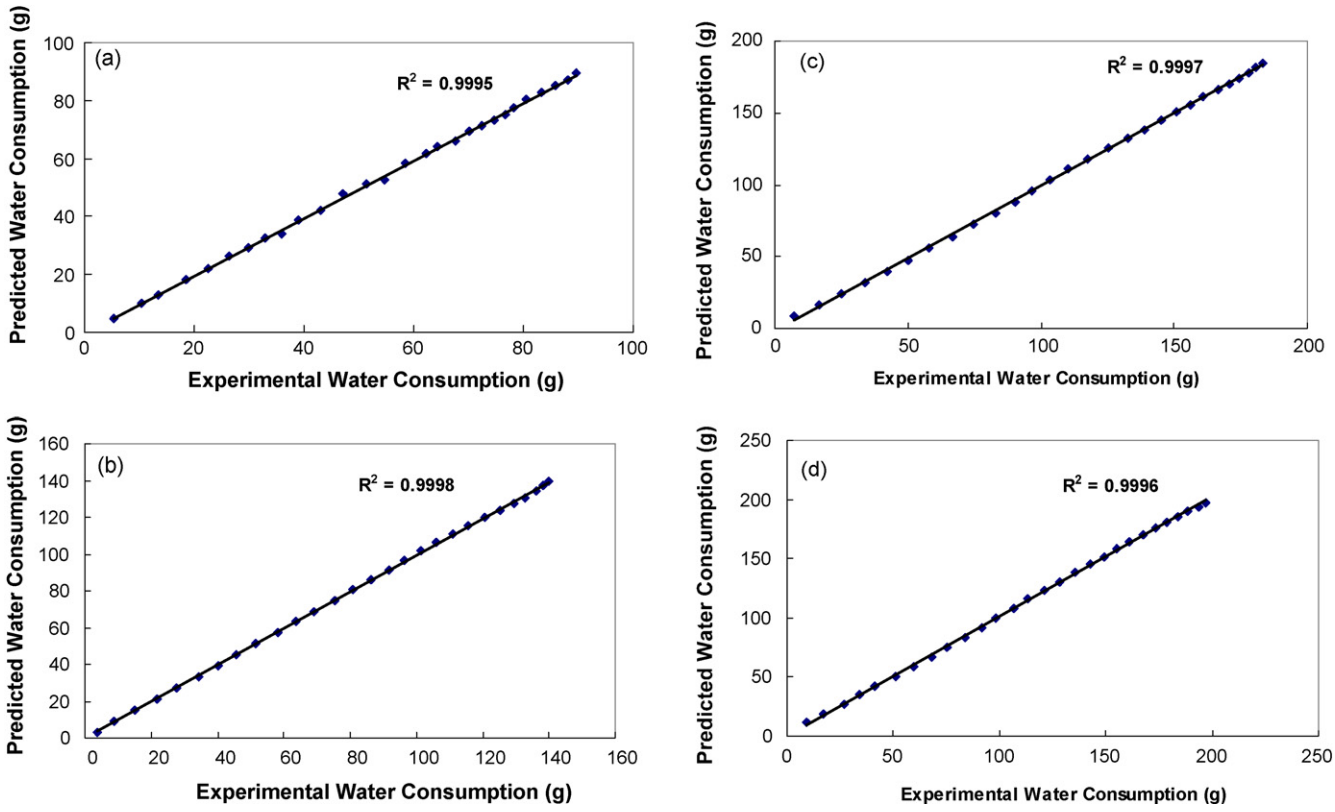

Fig. 7. Variations of predicted weights (water consumption quantity) vs. experimental weights (water consumption quantity) for network 3 in prediction set at 0–140 h for constant temperatures and voltages of (a) 30 °C and 15 V, (b) 60 °C and 14.25 V, (c) 80 °C and 14.25 V, (d) 80 °C and 14.75 V.

ibility with the corresponding experimental data. So, the model can be used with low prediction error in predicting of water consumption.

Fig. 8 illustrates test samples that validate the model (in three networks) at 0–140 h for constant temperatures and voltages of (a) 50 °C and 14.5 V, (b) 60 °C and 14.25 V, (c) 70 °C and 13.25 V. These samples represent data that have not taken part in the training; hence, they measure the network ability to replicate the correct response for any randomly drawn input. Fig. 9 shows the predicted time-water consumption behavior and

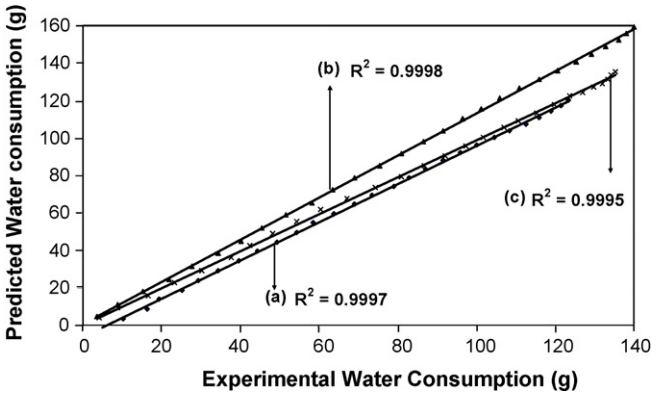

Fig. 8. Variation of weights (water consumption quantity) vs. experimental weights (water consumption quantity) for network 1, 2, and 3 at 0–140 h in validation data set, for constant temperatures and voltages of (a) 50 °C and 14.5 V, (b) 60 °C and 14.25 V, (c) 70 °C and 13.25 V.

experimental data for network 3 at 70 °C and constant voltages of (a) 13.25 V, (b) 14.25 V and (c) 15 V in validation set. Fig. 10 depicts the variation of predicted data versus experimental data for networks 1, 2 and 3 at different charge voltages, temperatures and times for ANN model in validation data set. As it is seen from Figs. 8–10 there are good agreements between results of predicted and experimental data in the validation datasets and this can verify the ability of this model. This model can be applied to other types of batteries as another application of it.

Table 6 shows maximum prediction error in prediction and validation sets. As it is seen from this table, there is a good agreement between experimental data and predicted data. The prediction error of 10% or lower is acceptable for ANN models. Although with increasing the number of layers and neurons, we can have the least error but it increases training time and decreases the speed of computation. Because of this we chose the minimum error that is acceptable in industrial applications.

Table 6
Mean prediction errors (%) of the proposed ANN model for prediction and validation sets

	Network		
	1	2	3
Prediction set	1.20	0.30	1.67
Validation set	0.99	0.03	0.76

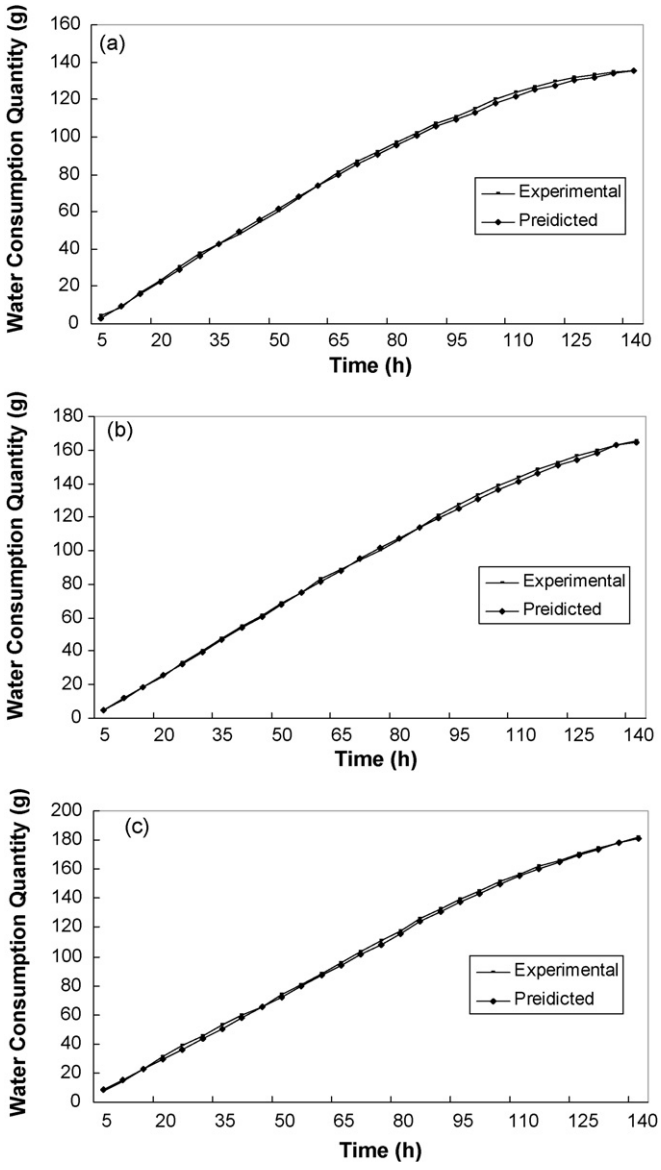

Fig. 9. Comparison of predicted time-water consumption behavior and experimental data for network 3 at 70 °C and constant voltages of (a) 13.25, (b) 14.25 and (c) 15 V in validation set.

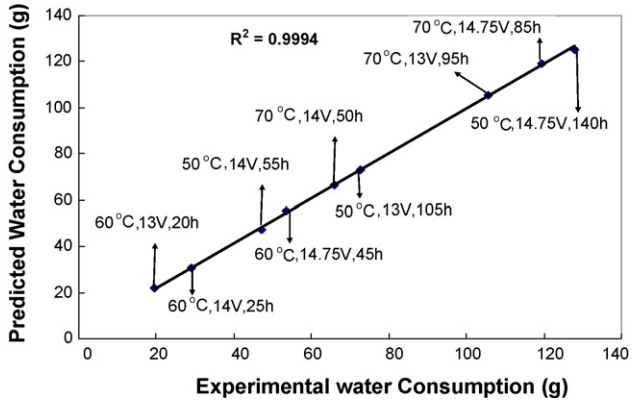

Fig. 10. Variation of predicted weights (water consumption quantity) vs. experimental weights (water consumption quantity) for networks 1, 2 and 3 at different charge voltages, different temperatures and times for ANN model in validation data set.

As mentioned before this network has two layers and the transfer function was tangent-sigmoid for the first layer and linear for the second one.

This model is compatible with different type of batteries in the antimony–lead-acid battery category with different capacities. To implement this model for different types of batteries, we should have three samples from the selected battery and record the result of water loss quantity in a short time (30 min) in one temperature and three voltages. When these data are imported to the network it can measure the amount of errors and adjust the model. Then, we can use the model for each temperatures or voltages.

With application of this model, long time of water consumption test (21–60 days according to different standards) is decreased to less than 1 h and certainly it can reduce the cost of test and save the time. While using this method, laboratory operators can do more tests and as a result each factory can follow the quality of its product more appropriately. Moreover the cost of energy is reduced in this model.

4. Conclusions

A water consumption computation model based on the artificial neural network (ANN) has been proposed. While compared to methods based on experimental data and standard calculation of water consumption, this method, based on the ANN, gives highly accurate estimation of water consumption quantity.

Accuracy and the generalization of the neural model in the system prediction are demonstrated by comparing test results with actual data.

The model can be used successfully for prediction of time-water consumption behavior at different constant temperatures and voltages. The final model was used in MATLAB 7 media for making a file (a program for water consumption prediction) for inexpert operators in industries of lead-acid batteries in order to predict water consumption quantity at any constant temperature and voltage.

Acknowledgement

We are deeply indebted to Professor Afsaneh Safavi for having provided us with indispensable suggestions and advice and to Payame-Noor University of Sirjan and Sepahan Battery Industrial Complex for their support.

References

[1] D. Linden, Handbook of Batteries, 3rd ed., McGraw-Hill, New York, 2001.
[2] J.H. Yan, H.Y. Chen, W.S. Li, C.I. Wang, Q.Y. Zhan, J. Power Sources 158 (2006) 1047–1053.
[3] T. Ohmae, K. Sawai, M. Shiomi, S. Osumi, J. Power Sources 154 (2006) 523–529.
[4] P. Ruetschi, J. Power Sources 127 (2004) 33–44.
[5] X. Muneret, V. Gobé, C. Lemoine, J. Power Sources 144 (2005) 322–328.
[6] D. Pavlov, V. Naidenov, S. Ruevski, V. Mircheva, M. Cherneva, J. Power Sources 113 (2003) 209–227.
[7] D. Linden, T.B. Reddy, Handbook of Batteries, 3rd ed., McGraw Hill, New York, 2002.
[8] H. Bode, Lead Acid Batteries, John Wiley, New York, 1977.

[9] IR http://www.dacs.dtic.mil/techs/neural.htm.
[10] J.B. Copetti, F. Chenlo, J. Power Sources 47 (1994) 109–118.
[11] P. Mauracher, E. Karden, J. Power Sources 67 (1997) 69–84.
[12] A.J. Salkind, C. Fennie, P. Singh, T. Atwater, D. Reisner, J. Power Sources 80 (1999) 293–300.
[13] A. Salkind, T. Atwater, P. Singh, S. Nelatury, S. Damodar, C. Fennie, D. Reisner, J. Power Sources 96 (2001) 151–159.
[14] V. Viswanathan, A.J. Salkind, J.J. Kellery, J.B. Ockerman, J. Appl. Electrochem. 25 (1995) 729–735.
[15] P. Singh, C. Fennie, D. Reisner, J. Power Sources 136 (2004) 322–333.
[16] C. Armenta-Deu, Renewable Energy 28 (2003) 1671–1684.
[17] M. Thele, S. Buller, D.U. Sauer, R.W. De Doncker, E. Karden, J. Power Sources 144 (2005) 461–466.
[18] M.T. Loponen, P. Jalas, J. Power Sources 30 (1990) 249–254.
[19] H. Karami, M.A. Karimi, M. Mahdipour, J. Power Sources 158 (2006) 936–943.
[20] IEC, 60095-1, Ed. 6, 2000-12.
[21] Peugeot Standard Systems, B255210, 2000.